Infrared spectroscopy of large scale single layer graphene on self assembled organic monolayer

Nak Woo Kim, Joo Youn Kim, Chul Lee, Sang Jin Kim, Byung Hee Hong, and E. J. Choi

Citation: Applied Physics Letters **104**, 041904 (2014); doi: 10.1063/1.4863416
View online: http://dx.doi.org/10.1063/1.4863416
View Table of Contents: http://scitation.aip.org/content/aip/journal/apl/104/4?ver=pdfcov
Published by the AIP Publishing

Infrared spectroscopy of large scale single layer graphene on self assembled organic monolayer

Nak Woo Kim,[1] Joo Youn Kim,[1] Chul Lee,[1] Sang Jin Kim,[2] Byung Hee Hong,[2] and E. J. Choi[1,a)]
[1]*Department of Physics, University of Seoul, Seoul 130-743, South Korea*
[2]*Department of Chemistry, Seoul National University, Seoul 151-742, South Korea*

(Received 30 August 2013; accepted 13 January 2014; published online 28 January 2014)

We study the effect of self-assembled monolayer (SAM) organic molecule substrate on large scale single layer graphene using infrared transmission measurement on Graphene/SAM/SiO_2/Si composite samples. From the Drude weight of the chemically inert CH_3-SAM, the electron-donating NH_2-SAM, and the SAM-less graphene, we determine the carrier density doped into graphene by the three sources—the SiO_2 substrate, the gas-adsorption, and the functional group of the SAM's—separately. The SAM-treatment leads to the low carrier density $N \sim 4 \times 10^{11}\,cm^{-2}$ by blocking the dominant SiO_2- driven doping. The carrier scattering increases by the SAM-treatment rather than decreases. However, the transport mobility is nevertheless improved due to the reduced carrier doping. © *2014 AIP Publishing LLC*.
[http://dx.doi.org/10.1063/1.4863416]

Graphene exhibits the high-mobility charge transport, near-perfect optical transparency, and the mechanical flexibility which are the highly useful properties for devices such as the transparent conductor and flexible display.[1–5] When graphene is deposited on the SiO_2/Si, the most common employed substrate, and operated at ambient conditions, it exhibits the p-type transport due to the hole carrier.[6–8] The hole is induced in the graphene partly by the unpaired Si- and O- dangling bonds of the SiO_2,[9] and also by the gas molecules such as H_2O and O_2 adsorbed on the graphene.[7,8] The carrier is scattered strongly by the SiO_2 substrate which is considered to limit the room-temperature mobility of graphene.[10–13]

Recently, thin layer of organic molecules is employed as new type of substrate for graphene.[14–18] When the SiO_2 substrate is exposed to vapor or liquid of the chemical agent, uniform molecular film of mono-layer thickness is formed spontaneously. One example of such self-assembled monolayer (SAM) molecules is depicted in Fig. 1 which consists of the silane Si-Cl base, (CH_2)n alkyl chain, and the end group such as CH_3. The SAM inactivates the Si- and O- dangling bonds of the SiO_2 protecting graphene from the substrate-driven carrier doping. Also now released from the direct contact with SiO_2, graphene may have weaker carrier scattering and consequently higher mobility. Previous transport measurements reported the I-V response of the graphene on the SAM/SiO_2/Si.[15–18] However, a systematic spectroscopy experiment could provide comprehensive understanding on the effect of the SAM-treatment on the carrier, which is still lacking.

In this work, we have performed the first infrared transmission measurement of the graphene deposited on the SAM-passivated SiO_2/Si substrate. In IR spectroscopy, the carrier density(N) and scattering rate(Γ) can be determined from the Drude response of graphene as shown by previous works.[19] We study two kinds of SAM's: First in the chemically inert CH_3-SAM, the molecular orbital of the CH_3 functional group are fully occupied with no unpaired electron.[15] The graphene transferred on it is doped mostly by the

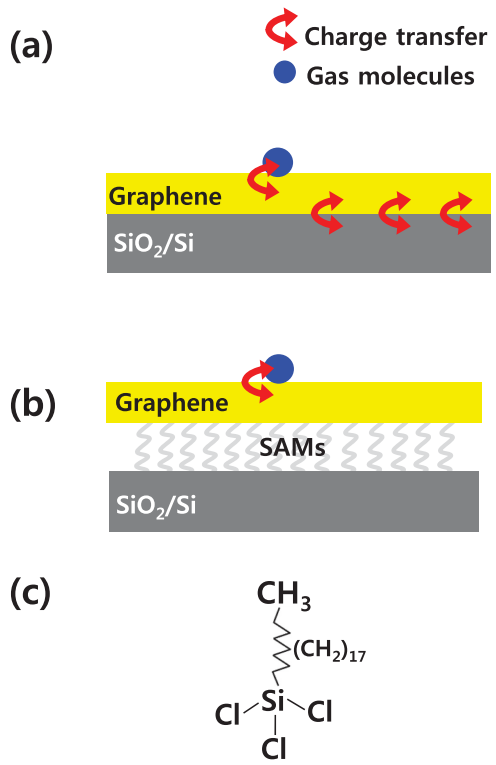

FIG. 1. Schematic illustration of the carrier doping into graphene. (a) on the SiO_2 substrate the carrier is doped in from the substrate and from the gas molecules adsorbed on the graphene. (b) on the CH_3-terminated SAM-layer the doping from the SiO_2 is blocked. (c) Molecular structure of the organic self assembled monolayer with the CH_3 end group.

a)echoi@uos.ac.kr

adsorbed gas with no doping from the SAM as sketched in Fig. 1. Second, in NH_2-SAM the NH_2 functional group has two unpaired electrons which can transfer into graphene.[15] If the transfer is large enough the graphene will show the electron-conduction (n-type) in contrast with the p-type conduction of the graphene on the bare SAM-less SiO_2/Si substrate. We measure the N's of the SAM-treated and untreated samples and determine the doping strength of the independent channels—from the SiO_2 substrate, the gas adsorbate, and the NH_2 functional group—separately.

Further, from the Γ's of the samples, we study the effect of the SAM-insertion on the carrier scattering. Eventually with the infrared N and Γ results, we explain the carrier mobility change of the SAM-treated CVD graphene.

The self assembled CH_3- and NH_2- monolayers were formed on SiO_2(300 nm)/p-Si by immersing the substrate in the reaction solution consisting of 10 mM of silane coupling agent and 10 ml of toluene for 3 h. Prior to the chemical treatment the ultrasonic-cleaned substrate was exposed to UV-Ozone for 20 min to activate the adhesion of the silanol group. As the silane agent Octadecyltrichlorosilane (ODTS) and 3-Aminopropyltriethoxysilane (APTS) were used for the CH_3-SAM and the NH_2-SAM, respectively. The large scale graphene was synthesized by the Cu-foil CVD method as described elsewhere[20,21] and transferred on the CH_3-SAM, NH_2-SAM, and the un-treated substrates. The graphene was selected from the same CVD batch and the transfer was made under the same chemical/ambient condition. Infrared transmission spectrum of the Graphene/SAM/substrate was measured using Fourier transform interferometer (FTIR-Bomem DA8) and bolometric detector at room temperature and 10^{-3} Torr of pressure. The transport current-voltage(I-V) curve was measured after the samples were fabricated into field effect transistor by evaporating the gold electrodes for the source/drain terminals and adding the indium(In) contact at the bottom of the p-Si for the electrostatic gating.

Figure 2(a) shows schematic diagram of the infrared transmission measurement. The IR intensity transmitted through Graphene/SAM/Substrate(=T_S) is normalized by that of SAM/Substrate(=T_R). Fig. 2(b) shows the relative transmittance $T(\omega) = T_S/T_R$ of the CH_3-SAM-treated graphene and the untreated graphene on the bare SiO_2/Si substrate. $T(\omega)$ decreases gradually as ω is decreased which represents the free carrier Drude absorption. In the CH_3-SAM graphene, the Drude strength is weaker than the untreated graphene implying that the carriers are less after the SAM-treatment. For quantitative understanding, we fit $T(\omega)$ using the multi-layer optical transmission analysis ReFit algorithm, where the graphene layer is modeled by the Drude conductivity

$$\sigma(\omega) = \frac{D}{\pi}\frac{1}{1 + i \times \frac{\omega}{\Gamma}}. \quad (1)$$

D and Γ are the Drude weight and the scattering rate, respectively. D is related with carrier density N as $D = \frac{v_F \cdot e^2}{\hbar}\sqrt{\pi N}$, where $v_F (= 1.1 \times 10^6\,\text{m/s})$ is the Fermi velocity. The fitting was performed using the ReFit program[22] with D and Γ as the variable parameters. Here, the coherent optical interference effects inside the SAM, SiO_2, and Si(incoherent) layers were rigorously taken into account. The details of the fitting procedure are described in Ref. 19. The fits (dashed curves) agree

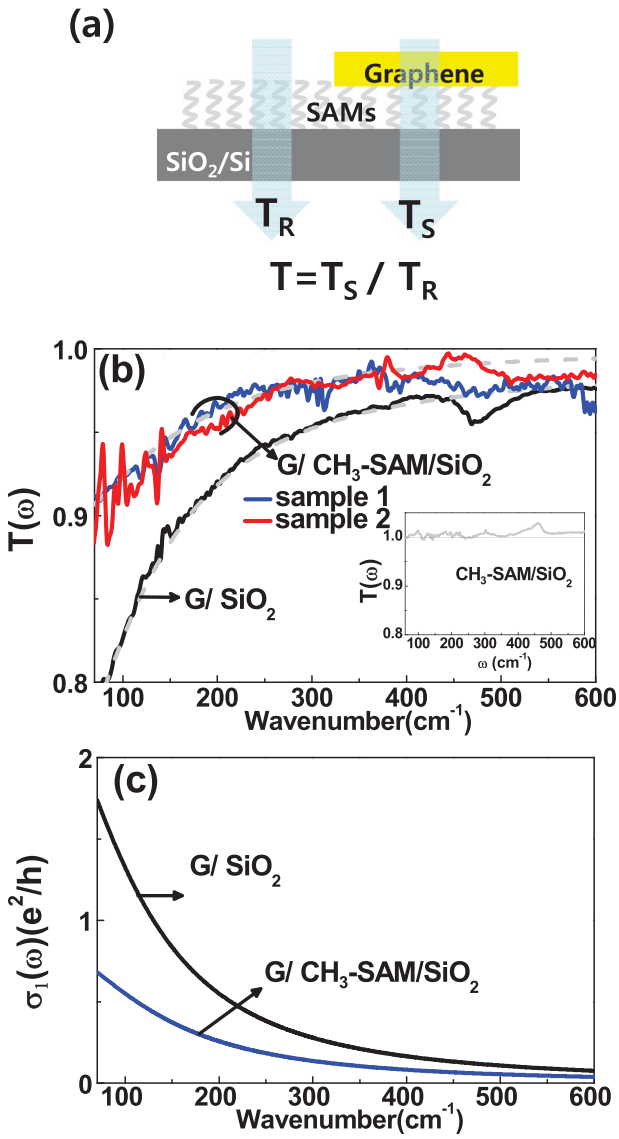

FIG. 2. (a) Schematic diagram of the infrared transmission measurement. The transmittance through the Graphene/SAM/Substrate(= T_S) is normalized by the transmittance through the SAM/Substrate(= T_R). (b) $T(\omega)$ of the CH_3-treated graphene (red/green curve) and the bare SiO_2-graphene (black). The dashed curves are the Drude model fits. Inset shows transmission of the CH_3-SAM/substrate referenced by that of the substrate. (c) Optical conductivity of graphene obtained from the Drude model fit.

TABLE I. Fitting results of the infrared Drude absorption for the SAM-treated and the bare, untreated graphene. D, Γ, and N represent the Drude weight, scattering rate, and the carrier density, respectively. μ_{IR} and μ_{tr} refer to the carrier mobility calculated from the IR-result and the transport I-V result.

Sample	D (cm^{-1})	Γ (cm^{-1})	N (cm^{-2})	μ_{IR} (cm^2/V s)	μ_{tr} (cm^2/V s)
Graphene/SiO_2	14 050	95	1.9×10^{12}	3770	3940
Grapehe/CH_3-SAM	9580	105	4.0×10^{11}	7340	7770
Grapehe/NH_2-SAM	9970	127	4.9×10^{11}	5600	6080

well with data. Figure 2(c) shows $\sigma_1(\omega)$, the real part of $\sigma(\omega)$, obtained from the fit. From the result of D (see Table I), we find $N_1 = 1.9 \times 10^{12}\,cm^{-2}$ and $N_2 = 4.0 \times 10^{11}\,cm^{-2}$ before and after the CH_3-treatment, respectively.

Before the SAM-passivation, graphene is doped by the two channels; the SiO_2 and the gas-adsorption leading to $N_1 = N_{SiO_2} + N_{ad}$, whereas after the SiO_2-channel is blocked by the CH_3-SAM passivation, N_2 is assigned to N_{ad}, $N_2 = N_{ad}$. From the two relations, we calculate $N_{SiO_2} = N_1 - N_{ad} = 1.5 \times 10^{12}\,cm^{-2}$. Note that N_{SiO_2} is larger than N_{ad} by $N_{SiO_2} \sim 4 \times N_{ad}$ which shows that 80% of the hole-carrier in Graphene/SiO_2/Si is coming from the substrate. This dominant doping channel can be removed by use of the CH_3-SAM which demonstrates that the SAM-treatment is an useful route toward the low-doped, free-standing like large scale graphene. The two numbers N_{ad} and N_{SiO_2} determined separately are useful for future application of the CVD graphene. The inset of Fig. 2(b) displays the IR transmission of the CH_3-SAM itself which is the normalized transmittance of the SAM/substrate and the substrate-only, T = T(SAM/substrate)/T(substrate). T does not show any Drude absorption in the measured frequency range supporting that the Drude signal we measured and analyzed is solely from the graphene.

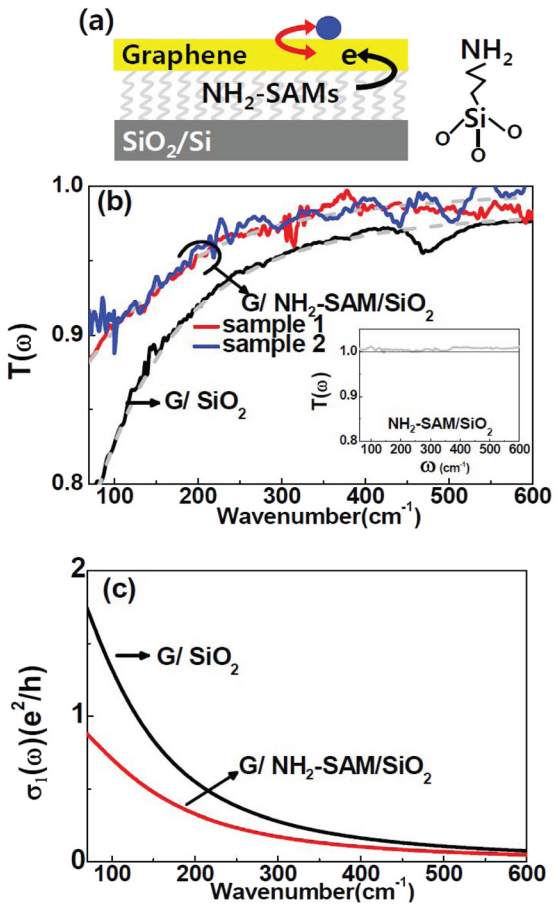

FIG. 3. (a)Schematic illustration of the doping routes for graphene on NH_2-SAM treated substrate. (b) Infrared transmission of the CVD graphene transferred on the NH_2-SAM modified substrate. The dashed curves represent the Drude model fit of the data. Inset shows the IR transmission spectrum of the NH_2-SAM only. (c) Optical conductivity of the graphene obtained from the Drude model fit.

In contrast with the CH_3-SAM, the chemically active NH_2-SAM can dope graphene with electron.[15] Fig. 3(a) shows the Drude response of the NH_2-SAM graphene. By fitting the data, we obtain $N = 4.9 \times 10^{11}\,cm^{-2} \equiv N_3$. The N_3 is result of the two dopings, $N_3 = N - N_e$, by the gas-adsorption N_{ad}(hole) and by the NH_2-group N_e(electron). The I-V curve (Fig. 4) shows that the NH_2-SAM has the n-type conduction as judged from the charge neutral voltage, implying that the electron doping is stronger, $N_{ad} < N_e$. We obtain N_e, the density of electron donated by the NH_2-SAM from $N_e = N_{ad} + N_3 = 8.9 \times 10^{11}\,cm^{-2}$. The average distance between the molecular chains of SAM is about 4.4 Å (Ref. 23) which corresponds to the 2D chain density $N_{chain} = 5.2 \times 10^{14}\,cm^{-2}$. The number of electron transferred from each NH_2-chain is therefore $n = \frac{N_e}{N_{chain}} = 1.7 \times 10^{-3}$ which is very weak compared with 2, the number of unpaired NH_2-electron. The charge transfer is determined by the intrinsic chemical potential difference between the graphene and the NH_2-SAM, and also extrinsically by the contact area between them. In CVD graphene, the imperfect contact due to the nano-ripple and graphene folding can hinder the electron transfer. If the contact is improved to bring the transfer efficiency to $n \sim 10^{-2(-1)}$, N_3 can increase to $\sim 10^{13(14)}\,cm^{-2}$ which shows that strong n-type graphene could be fabricated by the SAM substrate only without the complicated field-effect gating device fabrication.

Now, we study the mobility of the SAM-graphene. Fig. 4 shows the measured I-V curves of the three samples. Mobility μ is derived from the transport I-V data by[24,25]

$$\mu_{tr} = \frac{dI}{dV}\frac{L}{C_i V_D W}, \tag{2}$$

using the charge capacitance $C_i = 1.08 \times 10^{-8}\,F\,cm^{-2}$, the fixed source-drain voltage $V_D = 0.1\,V$. The length/width ratio(L/W) of the conducting channel was 1/1 for the SiO_2-sample, 1/1.7 for the CH_3-SAM, and 1/1.6 for NH_2-SAM, respectively. When the graphene is un-gated($V_g = 0$), the condition under which the IR data is taken, we obtain $\mu_{tr} = 3940\ cm^2/V\,s$ for the graphene on SiO_2, $\mu_{tr} = 7770\ cm^2/V\,s$ on CH_3-SAM, and $6080\ cm^2/V\,s$ on NH_2-SAM, respectively, where the subscript "*tr*" stands

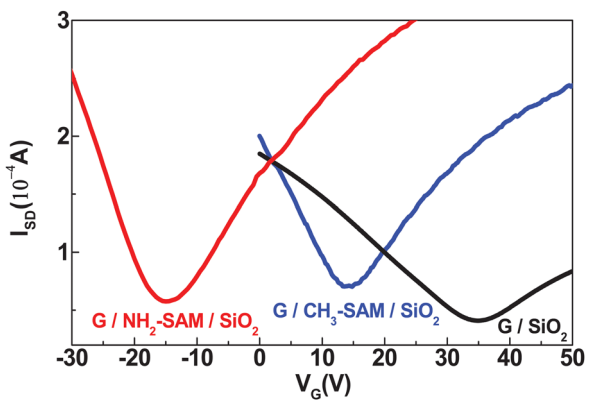

FIG. 4. I-V curve of CVD graphene transferred on CH_3-SAM, NH_2-SAM, and bare SiO_2/Si substrate.

for the transport mobility. In the mean time, the μ can be expressed in terms of the N and Γ as[24]

$$\mu = \left(\frac{e}{\sqrt{\pi}h}\right)\left(\frac{v_F}{\sqrt{N}}\right)\left(\frac{1}{\Gamma}\right). \quad (3)$$

We calculate μ using the N and Γ results of the Drude fit to find the infrared mobility $\mu_{IR} = 3770$ cm^2/V s (SiO_2), 7340 cm^2/V s (CH_3-SAM), and 5600 cm^2/V s (NH_2-SAM), respectively. μ_{IR} and μ_{tr} are in good agreement with each other showing the consistency between the two measurements. Here, we confirmed that the mobility and Drude conductivity show no change at the pressure $p = 10^{-3}$ Torr and ambient pressure under which the IR- and transport-data were taken, respectively.

The N, Γ, μ_{IR}, and μ_{tr} of the three samples are summarized in Table I. One should note that the scattering rate changes from $\Gamma = 95\,cm^{-1}$ (SiO_2) to $105\,cm^{-1}$ (CH_3), and $127\,cm^{-1}$(NH_2) showing that the carrier scattering is not reduced even after the graphene is liberated from the direct contact with SiO_2 substrate by the SAM's. Instead it increases due to some new scattering source from the SAM. μ is nevertheless enhanced because of N in Eq. (3) in the denominator which, as we discussed above, is much smaller in the SAM-graphene. The N-decrease is large enough to overcome the Γ, in spite that Γ even increases by the SAM, resulting in the notably higher μ. In this context, the doping control by use of the SAM-coverage on the SiO_2 is fruitful for the mobility improvement. However, search for a SAM material which reduces Γ, therefore can further enhance μ, is strongly needed. At room temperature, the surface polar phonon (SPP) of SiO_2 is considered to be a strong source of scattering which determines the mobility.[26,27] The SPP has the long-ranged Coulomb interaction nature, which is probably why the mono-layer molecule film is ineffective in reducing Γ.

To conclude, we have studied the carrier doping and the mobility of CVD graphene/SAM/SiO_2/Si samples from the contact-free infrared transmission measurement. Without the SAM-passivation of the SiO_2/Si substrate graphene is doped by the holes, 80% of them from the SiO_2 (density $N = 1.9 \times 10^{12}\,cm^{-2}$) and the rest 20% from the gas-adsorption ($N = 4 \times 10^{11}\,cm^{-2}$), respectively. By use of the chemically inert CH_3-SAM the dominant SiO_2—doping channel is blocked which brings the CVD graphene one step closer toward the ideal neutral graphene. In the NH_2-SAM, the efficiency of the electron doping from the NH_2-functional group is very weak ($n = 10^{-3}$) suggesting that highly n-type conduction would be possible if the graphene/SAM contact is increased. The transport mobility μ_{tr} and infrared mobility μ_{IR} show consistently that SAM-treatment improves the carrier mobility through the carrier density suppression.

We thank Keun Soo Kim for helping us with the sample preparation. This work was supported by NRF funded by the MEST (Grant No.2011-0029645). The work at SNU was supported by NRF funded by the MEST (Grant No. 2011-0031629).

[1]F. Bonaccorso, Z. Sun, T. Hasan, and A. C. Ferrari, Nature Photon. **4**, 611–622 (2010).
[2]A. K. Geim and K. S. Novoselov, Nature Mater. **6**, 183–191 (2007).
[3]J.-C. Charlier, P. C. Eklund, J. Zhu, and A. C. Ferrari, Carbon Nanotubes, Top. Appl. Phys. **111**, 673–709 (2008).
[4]P. R. Wallace, Phys. Rev. **71**, 622–634 (1947).
[5]M. Orlita, C. Faugeras, P. Plochocka, P. Neugebauer, G. Martinez, D. K. Maude, A. L. Barra, M. Sprinkle, C. Berger, W. A. de Heer, and M. Potemski, Phys. Rev. Lett. **101**, 267601 (2008).
[6]M. Ishigami, J. H. Chen, W. G. Cullen, M. S. Fuhrer, and E. D. Williams, Nano Lett. **7**, 1643–1648 (2007).
[7]F. Schedin, A. K. Geim, S. V. Morozov, E. W. Hill, P. Blake, M. I. Katsnelson, and K. S. Novoselov, Nature Mater. **6**, 652–655 (2007).
[8]S. Ryu, L. Liu, S. Berciaud, Y.-J. Yu, H. Liu, P. Kim, G. W. Flynn, and L. E. Brus, Nano Lett. **10**, 4944–4951 (2010).
[9]Y.-J. Kang, J. Kang, and K. J. Chang, Phys. Rev. B. **8**, 115404 (2008).
[10]J.-H. Chen, C. Jang, S. Adam, M. S. Fuhrer, E. D. Williams, and M. Ishigami, Nat. Phys. **4**, 377–381 (2008).
[11]E. H. Hwang and S. Das Sarma, Phys. Rev. B. **77**, 115449 (2008).
[12]S. V. Morozov, K. S. Novoselov, M. I. Katsnelson, F. Schedin, D. C. Elias, J. A. Jaszczak, and A. K. Geim, Phys. Rev. Lett. **100**, 016602 (2008).
[13]T. O. Wehling, M. I. Katsnelson, and A. I. Lichtenstein, Chem. Phys. Lett. **476**, 125–134 (2009).
[14]K. Yokota, K. Takai, and T. Enoki, Nano Lett. **11**, 3669–3675 (2011).
[15]J. Park, W. H. Lee, S. Huh, S. H. Sim, S. B. Kim, K. Cho, B. H. Hong, and K. S. Kim, J. Phys. Chem. Lett. **2**, 841–845 (2011).
[16]Z. Yan, Z. Sun, W. Lu, J. Yao, Y. Zhu, and J. M. Tour, ACS Nano **5**, 1535–1540 (2011).
[17]X. Wang, J.-B. Xu, C. Wang, J. Du, and W. Xie, Adv. Mater. **23**, 2464–2468 (2011).
[18]B. Lee, Y. Chen, F. Duerr, D. Mastrogiovanni, E. Garfunkel, E. Y. Andrei, and V. Podzorov, Nano Lett. **10**, 2427–2432 (2010).
[19]J. Y. Kim, C. Lee, S. K. Bae, K. S. Kim, B. H. Hong, and E. J. Choi, Appl. Phys. Lett. **98**, 201907 (2011).
[20]X. Li, W. Cai, J. An, S. Kim, J. Nah, D. Yang, R. Piner, A. Velamakanni, I. Jung, E. Tutuc, S. K. Banerjee, L. Colombo, and R. S. Ruoff, Science **324**, 1312 (2009).
[21]S. Bae, H. Kim, Y. Lee, X. Xu, J.-S. Park, Y. Zheng, J. Balakrishnan, T. Lei, H. R. Kim, Y. I. Song, Y.-J. Kim, K. S. Kim, B. Ozyilmaz, J.-H. Ahn, B. H. Hong, and S. Iijima, Nat. Nanotechnol. **5**, 574–578 (2010).
[22]A. B. Kuzmenko, E. van Heumen, F. Carbone, and D. van der Marel, Phys. Rev. Lett. **100**, 117401 (2008).
[23]A. Ulman, Chem. Rev. **96**, 1533–1554 (1996).
[24]V. Perebeinos and P. Avouris, Phys. Rev. B **81**, 195442 (2010).
[25]R. S. Shishir and D. K. Ferry, J. Phys.: Condens. Matter **21**, 232204 (2009).
[26]J.-H. Chen, C. Jang, S. Xiao, M. Ishigami, and M. S. Fuhrer, Nat. Nanotechnol. **3**, 206–209 (2008).
[27]S. Fratini and F. Guinea, Phys. Rev. B **77**, 195415 (2008).